

Pulse shape discrimination of CLYC, CLLBC and EJ-276 with SiPM readout

Bjoern Seitz^{1,*}, David Bennett¹, and Frank Thomson¹

¹SUPA School of Physics and Astronomy, University of Glasgow, Glasgow G12 8QQ, U.K.

(*) Bjoern.Seitz@glasgow.ac.uk

Abstract—Solid state detectors for the detection of thermal and fast neutrons find widespread applications. They often operate in a high gamma-radiation field or are required to discriminate between gamma-radiation and neutrons. Organic and in-organic scintillation materials are proposed as detector materials. These materials often exhibit different pulse shapes in their light output, which allows a variety of pulse shape analysis (PSA) techniques to be used to distinguish the two species of radiation. The current maturity of silicon based single photon counters (SiPM) provides a viable visible photon detector alternative to conventional vacuum based photo multiplier tubes (PMT). However, their impact on PSA has not been deeply studied. Three solid state scintillation materials, CLYC, CLLBC and EJ-276 are coupled to an array of SiPM and exposed to neutron and gamma radiation. Their response is characterized using a variety of PSA algorithms and quantified in a Figure of Merit. Conventional charge comparison algorithms perform well for all materials, while a Fourier component analysis shows particular strength for the in-organic materials tested.

Keywords —neutron detection, pulse shape analysis, SiPM, Fourier analysis, scintillation detectors

I. INTRODUCTION

THE detection of neutrons and the discrimination between neutrons and gamma-radiation finds widespread applications across a variety of fields, from evaluating additional dose in radiotherapy to scanning cargo to the monitoring of nuclear installations and the calibration of neutron sources or nuclear emitting radio-isotopes. Scintillation counters exhibiting different scintillation light pulse shapes, depending on the type of radiation detected are a promising solution meeting these requirements. The analysis of these pulse shapes (Pulse Shape Analysis (PSA)) provides the identification of each particle species, with several methods being available. In addition to the well established liquid scintillation materials, recent organic and in-organic solid state scintillation materials show great promise in detecting neutrons and discriminating these from gamma radiation.

In parallel, solid state visible light photon counters based on SPAD arrays have been developed and provide a rugged and compact alternative to conventional vacuum based Photo Multiplier Tubes (PMT). These Silicon Photo Multipliers

(SiPM) show a high photon detection efficiency, fast timing and acceptable levels of noise [1]. However, SiPM will exhibit non-linearities with increasing incident light level, raising questions about their suitability for use in pulse shape analysis applications.

The following text describes tests performed with two inorganic and one organic scintillator coupled to an SiPM array and exposed to thermal and fast neutrons in the presence of a gamma radiation field. The detector response was studied on a wave-form level and analyzed using a variety of pulse shape analysis algorithms. Section II describes the materials and experimental setup. The PSA and performance metrics used to compare the different materials is detailed in section III. Section IV summarizes the results and provides a conclusion.

II. EXPERIMENTAL SETUP AND METHODS

The detector system tested consists of the scintillator material under test coupled to a SiPM array via a custom light guide and read out via a custom front-end board and a commercial waveform digitizer to record the full pulse shape for each event. An example of the constructed detector system is shown in fig. 1 below.

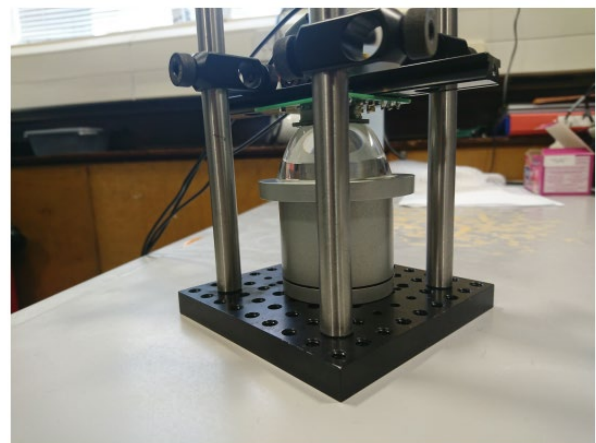


Fig. 1. Photograph of the detector setup used for these tests. The grey cylinder houses the scintillation material. Above it, the custom pulse shape preserving light guide is visible, followed by the electronics board housing the SiPM array.

The three materials tested were two inorganic crystals, CLYC ($\text{Cs}_2\text{LiYCl}_6:\text{Ce}$) [2,3] and CLLBC ($\text{Cs}_2\text{LiLa}(\text{Br},\text{Cl})_6:\text{Ce}$), and one organic material, EJ-276. The inorganic crystals provide a good sensitivity to thermal neutrons through capture reactions on ^6Li and ^{35}Cl . Their

average density is comparable with NaI:Tl and they are expected to perform better than this in terms of gamma detection efficiency and resolution. Both inorganic crystals are expected to exhibit clear pulse shape differences between neutron and gamma radiation. In contrast, E-276 is not expected to provide a good response to gamma radiation, but an excellent response to fast neutrons from collisions with the material's protons [4,5].

Each scintillator was constructed as a rect-cylinder with 51 mm diameter and 51 mm height. All three detector materials are packaged and sealed in a cylindrical aluminum housing with reflective coating on the inside and a quartz or perspex window for the inorganic and organic scintillators respectively. A pulse shape conserving light guide made from PMMA was constructed to couple the circular exit surface of the scintillator to a square 8x8 array of SensL J 30035 SiPM. The individual SiPM have a size of 3mm x 3mm. Each individual SiPM consists of 5676 $3.07\mu\text{m} \times 3.07\mu\text{m}$ pixels. The maximum photon detection efficiency is given as 38% at 420 nm with an overvoltage of $V=2.5V$ and 50% at $V=6V$. The array was operated at a common voltage of 30V. This corresponds to a setting of 5V above the established breakdown voltage. The analog signals of the individual SiPM were summed on a custom PCB and fed to a CAEN DT5730B waveform digitizer. A schematic of the setup is shown in fig. 2. It should be noted that throughout the experiment, the source configuration, light transport, light detection and read-out electronics have been kept constant. Coupling a different scintillation crystal was the only change.

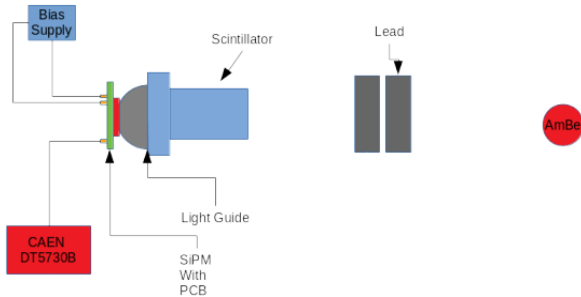


Fig. 2. Schematics of the test setup depicted as a photograph in fig.1. The SiPM array is shown coupled to the pulse-shape conserving light guide coupled to the scintillator under test. A lead shield shield the detector from gamma radiation emitted from the AmBe neutron source. The detector is powered by a LV bias supply and read out by a CAEN DTS5730B waveform digitizer.

Neutrons were generated using an AmBe source through α -capture on ^9Be . This results in the emission of a fast neutron and the emission of a gamma ray with an energy of $E_\gamma = 4.4$ MeV. The branching ratio for this reaction is 55%. The emitted neutrons have a maximum neutron energy E_n of $E_n=11$ MeV, with a mean unmoderated energy between $4 \text{ MeV} < E_n < 5$ MeV. Paraffin was used to moderate neutrons to thermal energies when desired and substantial lead shielding was employed to limit the flux of gamma radiation into the detector when needed.

The data were collected from the CAEN DT5730B waveform digitizer and stored directly in waveform format for

further analysis.

III. PULSE SHAPE ANALYSIS AND PERFORMANCE METRIC

All scintillator prototypes were examined with identical experimental setups. Three different methods of PSA were used and a figure of merit calculated to allow a direct comparison of the different materials and algorithms.

A. Charge comparison method

One of the longest established method which was even realized in analog electronics is the charge comparison method. As illustrated in Fig 3, taken from a measurement using stilbene as scintillator material, the scintillation pulse created by gamma radiation has a similar rise time, but much faster fall time compared to the scintillation pulse created by neutrons.

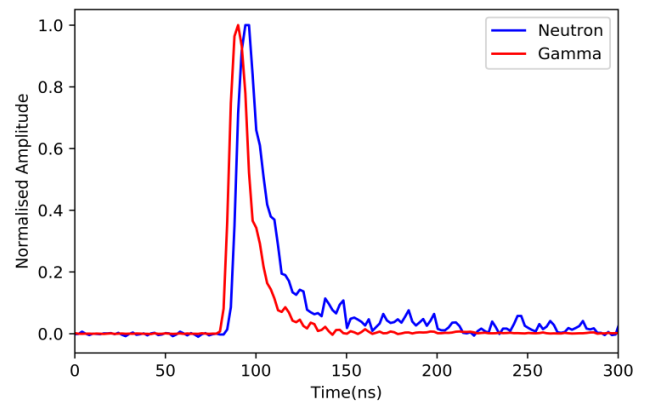


Fig. 3. Recorded waveforms measured using a Stilbene crystal exposed to radiation from an AmBE source. A clear distinction in pulse rise time and pulse fall time is visible in the signal from both radiation species. These pulse shape differences can be exploited in PSA to identify each particle species..

A measured pulse will be integrated over two different time periods, the short gate and the long gate. In the case of a short, fast pulse, these two pulse integrals will be very similar, while in the case of a pulse with a slow decay time, the integral over the longer gate will yield a significantly larger value. Defining a value PSD using the integrated charge over the short gate Q_1 and the long gate Q_2 , a discrimination variable between the two particle species can be defined as

$$PSD = 1 - \frac{Q_1}{Q_2}$$

When this value is plotted as a function of the total energy deposited inside the scintillator volume, a separation between the two particle species is clear visible, as shown in Fig. 4 taken from a measurement of Stilbene exposed to thermal neutrons from an AmBe source.

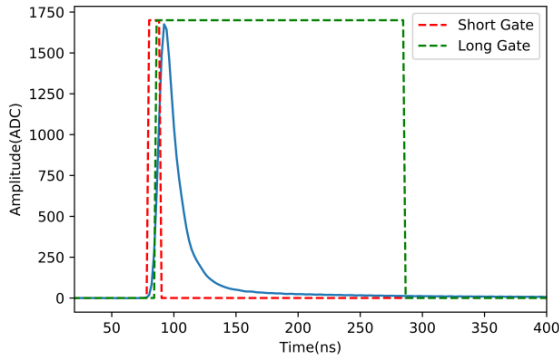


Fig. 4. Illustration of the charge comparison method for a pulse emitted by a stilbene scintillator irradiated by neutrons. The boxes indicate the integration regions for short and long pulse gates providing the charge integral Q_1 and Q_2 used for PSA.

B. Fourier component analysis

The use of a waveform digitizer provides access to the full waveform, allowing a wider form of analysis to be performed. Most PSA algorithms are performed in the time domain. The full access to the waveform allows PSA to be performed in the frequency domain as well [6,7]. This type of method offers several advantages over time domain based methods, as it mitigates many of the effects of noise common in scintillation signals by reducing the dependence on the timing aspects of the signal.

One particular method in the frequency domain is provided by a simple Fourier transform of the signal, greatly simplifying the deconvolution of the signal for an affordable computational cost. In many cases, a simple comparison of the amplitudes in the high frequency (HF) and low frequency (LF) domains for the Fourier transform may be sufficient. As the zeroth component is equal to the integral of the entire signal in the time domain, the comparison of the zeroth and first order component can be considered equivalent to the charge comparison methods. As such, the PSD factor is given as the ratio of the sum over all Fourier components starting with the first order component over the sum of all Fourier components starting at zeroth order, yielding a range of $0 < PSD < 1$.

C. Risetime method

The risetime method is a variant of the charge comparison method in that it tries to exploit not the fall time differences, but differences in the risetime of the scintillation light pulse due to the different scintillation mechanisms for neutrons and gamma rays [8]. In this method, the time it takes a pulse to reach a set fraction of the maximum pulse height is measured. The data presented here compare the risetime between 20% and 80% of the pulse. Cheers This method could also be realized in analog electronics, while this study uses a full software implementation of the algorithm. A PSD value is defined from the fractions of the leading edge in a CFD algorithm f_1 and f_2 as

$$PSD = -1/2 \left(\left(\frac{t1}{\log(1-f1)} \right) + \left(\frac{t2}{\log(1-f2)} \right) \right).$$

D. Figure of Merit

In order to compare different detector materials and different PSA algorithms, a metric has to be introduced to measure their relative performance on an equal footing. As outlined above, the scintillation crystal was the only variable during the experiment. The metric used in this comparison follows the well established definition of a Figure of Merit (FoM) for two variables with reasonably distinct (ideally Gaussian) distributions. It is assumed that the distribution of the aforementioned PSD factors for the two particle species is Gaussian in shape. The FoM is then defined as the ratio of the separation S of the mean value of the two distributions divided by the sum of their individual full width at half maximum, d_1 and d_2 :

$$FoM = \frac{S}{d_1 + d_2}.$$

The larger the FoM value, the better the detector performance, with values $FoM < 1$ signifying a strong overlap of the two distributions and values of $FoM > 3$ showing a complete separation. A FoM of 1 is considered a good separation [9].

IV. RESULTS

Three materials were exposed to fast and moderated neutrons emitted from an AmBe source. The light collection, detection and read-out was kept the same for all experiments. The three described PSA algorithms were applied to the recorded waveforms.

A. CLYC:Ce

CLYC:Ce is an inorganic scintillation material with strong pulse shape differences between thermal neutrons and gamma radiation. Given that most neutron detection relies on capture reactions, it's performance when detecting fast neutrons is expected to be poor. Fig. 5 shows the conventional PSA using charge comparison when CLYC:Ce is exposed to thermal neutrons in the presence of a gamma radiation field.

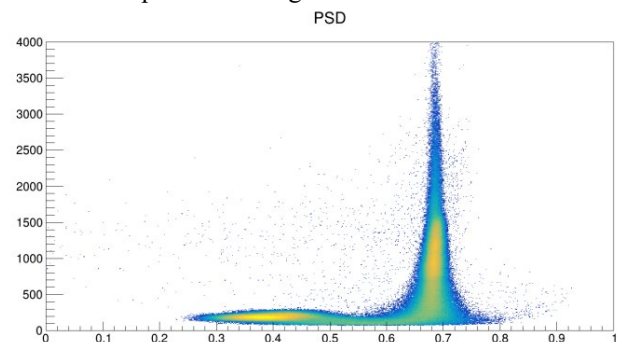


Fig. 5. Heatmap showing the distribution of the PSD variable on the x-axis versus the distribution of uncalibrated ADC channels representative of the total energy deposited in the scintillation volume on the y-axis for a CLYC:Ce crystal exposed to radiation from an AmBe source. A clear separation of the two particle species is visible. The PSD variable is calculated as described in the section on the charge comparison method.

A clear distinction between the two particle species is visible. The FoM was calculated to be 2.77. CLYC:Ce also showed an excellent FoM when the signals were analyzed using the HF Fourier method, yielding an FoM of 10.98. The corresponding heat map is shown in Fig. 6. An analysis with the LF Fourier component does not work well, with an FoM of 0.61. The risetime method yields an FoM of 1.77.

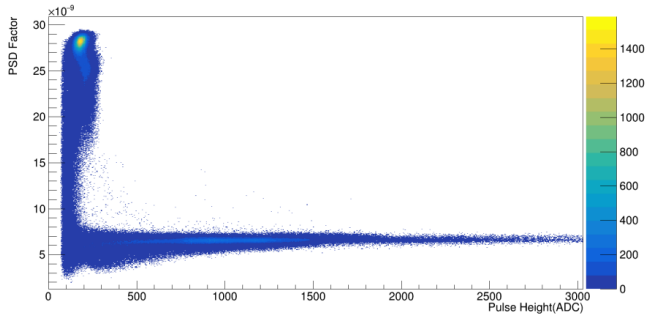


Fig. 6. Heatmap showing the distribution of the PSD variable on the y-axis versus the distribution of uncalibrated ADC channels representative of the total energy deposited in the scintillation volume on the x-axis for a CLYC:Ce crystal exposed to radiation from an AmBe source. The PSD variable is calculated for the HF Fourier method. A clear separation of the two particle species is visible.

B. CLLBC:Ce

Like CLYC:Ce, CLLBC:Ce is expected to work very well for thermal neutrons given its predominant mode of neutron detection via capture reactions. The slightly higher density should result in a better gamma detection efficiency. CLLBC:Ce shows a significantly better discrimination between neutrons and gamma radiation compared to CLYC:Ce in the charge comparison method with a FoM of 3.69. The corresponding spectrum is shown in Fig. 7.

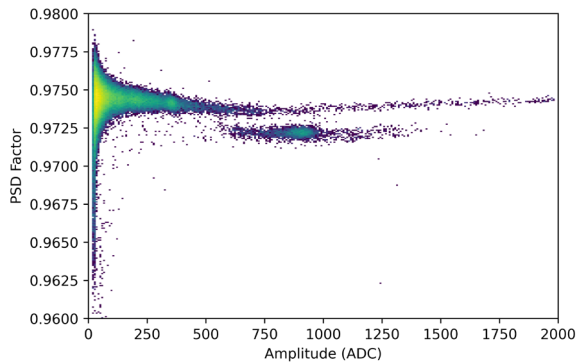


Fig. 7. Heatmap showing the distribution of the PSD variable on the y-axis versus the distribution of uncalibrated ADC channels representative of the total energy deposited in the scintillation volume on the x-axis for a CLLBC:Ce crystal exposed to radiation from an AmBe source. A clear separation of the two particle species is visible. The PSD variable is calculated as described in the section on the charge comparison method.

Due to an equipment malfunction, the HF Fourier method and the risetime method could not be evaluated. However, the LF Fourier method, depicted in Fig. 8 shows significant promise with a FoM of 4.1, exceeding the performance of the classical charge comparison method.

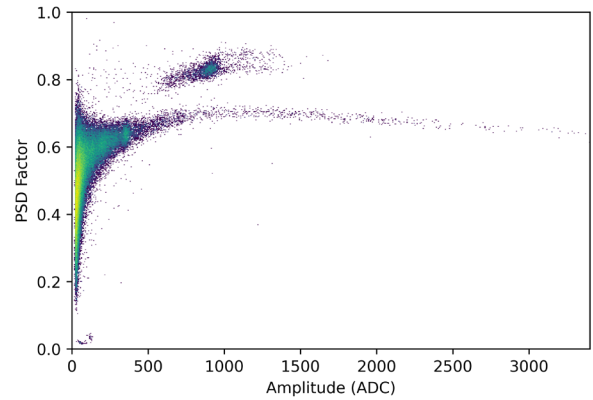


Fig. 8. Heatmap showing the distribution of the PSD variable on the y-axis versus the distribution of uncalibrated ADC channels representative of the total energy deposited in the scintillation volume on the x-axis for a CLLBC:Ce crystal exposed to radiation from an AmBe source. The PSD variable is calculated for the LF Fourier method. A clear separation of the two particle species is visible.

C. EJ-276

EJ-276 is, in contrast to CLYC:Ce and CLLBC:Ce an organic scintillator. Given the low density and low average atomic number, its performance in the detection of gamma radiation is expected to be poor. The material should also be better suited to faster neutrons and show some weakness in the detection of thermal neutrons. This is indeed observed, e.g as shown in Fig. 9 for the charge comparison method, yielding a FoM of only 0.85.

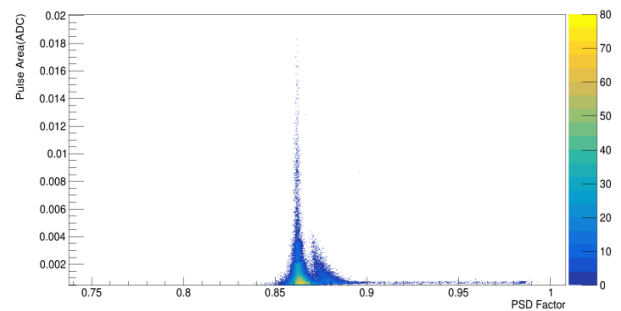


Fig. 9. Heatmap showing the distribution of the PSD variable on the x-axis versus the distribution of uncalibrated ADC channels representative of the total energy deposited in the scintillation volume on the y-axis for a EJ-276 scintillator exposed to radiation from an AmBe source. Only a poor separation of the two particle species is visible. The PSD variable is calculated as described in the section on the charge comparison method.

The LF Fourier component analysis failed to yield a measurable discrimination at all. The risetime component is also not promising, with a FoM of 0.57. An improvement, as with all investigated materials, can be seen in the frequency domain as shown in Fig. 10. The corresponding FoM is 1.19, showing a satisfactory separation between neutrons and gamma radiation.

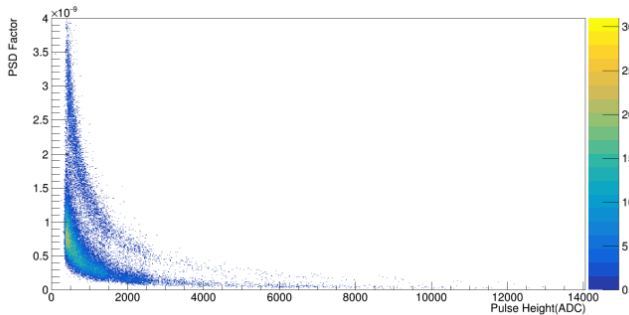


Fig. 10. Heatmap showing the distribution of the PSD variable on the y-axis versus the distribution of uncalibrated ADC channels representative of the total energy deposited in the scintillation volume on the x-axis for a EJ-276 scintillator exposed to radiation from an AmBe source. The PSD variable is calculated for the HF Fourier method. A satisfactory separation of the two particle species is visible.

V. SUMMARY AND CONCLUSION

Three solid state scintillation crystals with pulse shaping capabilities have been tested using fast and thermal neutrons in the presence of a gamma radiation field. These scintillators have been coupled to an array of SiPM readout by a waveform digitizer, allowing a variety of offline PSA algorithms to be applied to discriminate between neutron and gamma radiation. Two inorganic crystals, CLYC and CLLBD, have been tested in comparison with an organic scintillator, EJ-274.

A figure of merit has been introduced to compare the performance of each detector material and each PSA algorithm. The results are summarized in Table II. The performance of the inorganic crystals CLLBC and CLYC using the charge comparison method when exposed to thermal neutrons yields a FoM of 3.69 and 2.77 respectively. As expected from the material properties, the response of EJ-276 to thermal neutrons is worse, yielding a FoM of 0.85. This can be significantly improved by using different analysis techniques, most notably the HF Fourier component analysis, which increases the FoM for EJ-276 to 1.19 and for CLYC to 10.98. For technical reasons, the HF Fourier component analysis for CLLBC could not yet be performed, but the LF Fourier component analysis also shows an improvement yielding a FoM of 4.1. It is illustrative to compare the performance of Fourier transform methods in the case of CLYC and EJ-276. In both cases, the HF Fourier component method provided significant improvements, while the LF Fourier component analysis provided a poor result (FoM of 0.611) for CLYC and failed to provide a separation for EJ-276, indicating that great care has to be taken to optimize each analysis algorithm to the detector material at hand.

In summary, it could be shown that coupling a scintillator exhibiting pulse shape characteristics to an array of SiPM yields a capable neutron detector with strong neutron/gamma discrimination. The performance of each detector material was found to be within expectations, i.e. EJ-276 as an organic scintillator excelled for fast neutrons, while being significantly outperformed by both in-organic scintillation crystals for thermal neutrons.

The introduction of a waveform digitizer allows the study and optimization of a variety of PSA algorithms which, with

sufficient care will yield the best performance of a specific detector and read-out combination.

REFERENCES

- [1] D. Renker, "Geiger-mode avalanche photodiodes, history, properties and problems," *Nuclear Instruments and Methods in Physics Research A*, vol. 567, pp. 48–56, 2006.
- [2] N. D'Olympia, P. Chowdhury, C. Lister, J. Glodo, R. Hawrami, K. Shah, and U. Shirwadkar, "Pulse-shape analysis of CLYC for thermal neutrons, fast neutrons, and gamma-rays," *Nuclear Instruments and Methods in Physics Research Section A: Accelerators, Spectrometers, Detectors and Associated Equipment*, vol. 714, pp. 121–127, jun 2013.
- [3] A. Giaz, L. Pellegrini, F. Camera, N. Blasi, S. Brambilla, S. Ceruti, B. Million, S. Riboldi, C. Cazzaniga, G. Gorini, M. Nocente, A. Pietropaolo, M. Pillon, M. Rebai, and M. Tardocchi, "The CLYC-6 and CLYC-7 response to γ -rays, fast and thermal neutrons," *Nuclear Instruments and Methods in Physics Research, Section A: Accelerators, Spectrometers, Detectors and Associated Equipment*, vol. 810, pp. 132–139, 2016.
- [4] C. Liao and H. Yang, "Pulse shape discrimination using EJ-299-33 plastic scintillator coupled with a Silicon Photomultiplier array," *Nuclear Instruments and Methods in Physics Research, Section A: Accelerators, Spectrometers, Detectors and Associated Equipment*, vol. 789, pp. 150–157, 2015.
- [5] E. Van Loef, G. Markosyan, U. Shirwadkar, M. McClish, and K. Shah, "Gamma-ray spectroscopy and pulse shape discrimination with a plastic scintillator," *Nuclear Instruments and Methods in Physics Research, Section A: Accelerators, Spectrometers, Detectors and Associated Equipment*, vol. 788, pp. 71–72, 2015.
- [6] M. J. Safari, F. A. Davani, H. Afarideh, S. Jamili, and E. Bayat, "Discrete Fourier Transform Method for Discrimination of Digital Scintillation Pulses in Mixed Neutron-Gamma Fields," *IEEE Transactions on Nuclear Science*, vol. 63, no. 1, pp. 325–332, 2016.
- [7] G. Liu, M. J. Joyce, X. Ma, and M. D. Aspinall, "A digital method for the discrimination of neutrons and γ rays with organic scintillation detectors using frequency gradient analysis," *IEEE Transactions on Nuclear Science*, vol. 57, no. 3 PART 3, pp. 1682–1691, 2010.
- [8] B. D'Mellow, M. Aspinall, R. Mackin, M. Joyce, and A. Peyton, "Digital discrimination of neutrons and γ -rays in liquid scintillators using pulse gradient analysis," *Nuclear Instruments and Methods in Physics Research Section A: Accelerators, Spectrometers, Detectors and Associated Equipment*, vol. 578, pp. 191–197, 2007.
- [9] G. Ranucci, "An analytical approach to the evaluation of the pulse shape discrimination properties of scintillators," *Nuclear Instruments and Methods in Physics Research Section A: Accelerators, Spectrometers, Detectors and Associated Equipment*, vol. 354(2-3), pp. 389–399, 1995.